Desalination and Water Treatment
www.deswater.com
1944-3994/1944-3986 © 2012 Desalination Publications. All rights reserved
doi: 10.1080/19443994.2012.719660
50 (2012) 285–293
December
Taylor & Francis
Taylor & Francis Group

Impact of solution hydrodynamics on the deposition of $CaSO_4$ on brass

Abdul Quddus*, Luai M. Al-Hadhrami

Research Institute, King Fahd University of Petroleum & Minerals, P.O. Box 1524, Dhahran 31261, Saudi Arabia
Tel: +966 (3) 8603533; Fax: +966 (3) 8603996; email: amquddus@kfupm.edu.sa

Received 4 September 2011; Accepted 5 June 2012

ABSTRACT

An investigation was conducted to study the impact of solution hydrodynamics on the deposition of calcium sulfate scale on commercial brass by using a rotating cylinder electrode system at various pre-set rotational speeds, at 60 and 70°C on 120 and 600 grits polished cylindrical specimens. The effects of temperature, surface roughness, and flow conditions on the deposition of calcium sulfate scale on brass are presented. The results indicate the influence of solution hydrodynamics on the rate of calcium sulfate scale deposition on brass specimens by delineating the competing effect between the scale deposition and scale removal process that is occurring simultaneously under the fluid flow conditions generated in the study. The morphology of deposited crystals was obtained from scanning electron microscope (SEM) micrographs and composition was determined with energy dispersive X-ray spectrometer (EDS) method. The SEM analysis revealed prismatic needle- and rod-like crystals growth structure at nucleation sites branching out randomly over the substrate. The secondary growth on the already existing primary crystals of $CaSO_4$ was also noticed. The EDS analysis confirmed the composition of crystals comprising of Ca, S, and O as expected because of the purity of chemicals used.

Keywords: Scale; Calcium sulfate scale; $CaSO_4$; Hemihydrate; Gypsum; Brass; $CaSO_4$ on brass; Rotating cylinder electrode; RCE

1. Introduction

Accumulation of undesired superfluous mineral species from process fluids on heat transfer surface(s), is called scaling/fouling. The heat exchanger fouling alone is a major economic loss accounting to about 0.25% of the total gross domestic product in highly industrialized countries [1] and potentially remains a serious problem for the processing industries worldwide. The mechanically resilient, strongly adhering and undissolvable scale deposits cause process disruptions, frequent shutdowns, and sometimes catastrophic failures. The corrosion products, particulate matters, bio-mass, sludge and slime deposits are additional serious problems encountered by process industries. The reduction in thermal efficiency of the heat transfer equipment, disruption of process operations, loss of production, and economic losses are the gross consequences of these unwanted deposits. Scaling of tubes substantially reduces their ability to exchange heat effectively in heat exchangers and in desalination plants, the scale deposits affect both the quality and quantity of desalted brine water. In oilfield wells and surface facilities, the deposition of alkaline earth elements such as sulfates and carbonates of magnesium, calcium, barium, and strontium

*Corresponding author.

restrict flow through tubing strings and hence drastically decrease oil production. Therefore, the decrease in thermal efficiency and/or loss of production results in decline of revenues [2,3]. Moreover, the conjoint effect of scale and corrosion remains as challenging issues for the designers as well as operators throughout the lifecycle of a plant [4].

Laboratory methods to study scale deposition generally involve: (a) static experiments using glassware [3,5–7] and (b) dynamic experiments, involving once through or re-circulating flow loops [3,8–12]. Static experiments are easy to perform and seeded growth of crystals can also be achieved [6,7] easily. Static experiments are useful as they provide first approximation of scaling conditions. The hydrodynamic flow loops simulate industrial situations but are cumbersome to perform and require rigorous monitoring as well as copious volume of feed solution.

An easy alternative is the use of rotating cylinder electrode (RCE) or rotating disk electrode (RDE) systems. The RCE and RDE techniques are well-established methods for studying kinetics of corrosion [13–17] and electro-deposition [18,19]. These techniques have been utilized for the study of scale deposition [20–29] to a limited extent.

The RCE is geometrically analogous to pipe surface, and the cylindrical shape of RCE specimen renders comparatively more surface area than a round flat disc. Considering these advantages being appropriate, we chose RCE for our experimental study for the assessment of the rate of scale deposition compared to RDE. No electrochemical aspects were studied in the present work; therefore, only the scale deposition results obtained on brass substrate, using RCE under fluid flow conditions are presented with various other parameters of interest.

Neville et al. [25–27] studied the electrochemical aspects of surface/solution interactions for $CaCO_3$ scale growth and inhibition on a RDE made from SS-316L at different rotational speeds. They utilized a well-known oxygen reduction electrochemical technique to assess the formation of scaling on the RDE surface. They showed that the presence of scaling on the samples actually reduced the electroactive surface area of the specimen and the resulting electrochemical current response. With this technique, they found a good correlation between the surface coverage due to scale and the image analysis performed on the surface of scaled and un-scaled samples. They concluded that with the help of this technique, the mechanism of scale formation, and assessment of inhibitors and their interactions on the solid surface can be studied.

Morizot et al. [28] used the technique developed by Neville [25] to study the inhibition of $CaCO_3$ scale on an SS-316 rotating disc electrode surface. They used polyacrylic acid (PAA) as scale control inhibitor to inhibit both bulk precipitation and scale formation on the metal surface, in varying dosages. They evaluated the performance of PAA-inhibitor by the electrochemical technique and found that the efficacy of the inhibitor may be quite varying in relation to the surface deposition and bulk precipitation in the scaling solution.

Chen et al. [29] utilizing the electrochemical technique suggested by Neville et al. [25], studied the $CaCO_3$ scale formation on a RDE surface by using three different supersaturated scaling solutions. They showed that the formation of scale on the specimen and the precipitation in the bulk solution are two different processes which depend on the index of supersaturation. Under potentiostatic control, they monitored the surface coverage of the RDE due to scaling. The rate of oxygen reduction and the resulting electrical current diminished with time during their experiments which allowed ascertaining the presence of scaling on the surface of RDE samples while operating the RDE set-up.

Laboratory analyses and characterization conducted on the actual scale samples obtained from oil production fields of Arabian Gulf region by Singh and Abbas [30] showed that calcium sulfate, strontium sulfate, barium sulfate, and calcium carbonate are the most commonly found scales in production facilities of the Gulf region.

The deposition of barium sulfate, calcium sulfate, and calcium carbonate scales obtained by using RCE equipment was reported earlier [20–24]. The present work further reports the results of calcium sulfate scale hydrodynamically deposited on commercial brass substrate. The effect of temperature and surface roughness at various Reynolds numbers for calcium sulfate scale on brass substrate is highlighted.

Scale deposition is a complex process, involving many factors, such as: adequate solution supersaturation, temperature, pressure, hydrodynamic conditions of fluid flow system, etc. Nonetheless, hydrodynamics considerably has an important impact on the scale deposition process among these. Therefore, the basic understanding of scale formation and deposition process is vital for an effective water treatment and scale sequestration program.

The main impetus for the present investigation was to understand the deposition of mineral scales on commercial grade metallic materials available in the market. Brass, being a metal of interest used in the process industries, was selected as a substrate for calcium sulfate scale deposition. The commercial grade brass is an alloy of 70% Cu and 30% Zn, usually

known as alpha-brass. Moreover, the experimental parameters used in the study are representative of the process industries operating conditions.

2. Experimental

A schematic of an EG&G Princeton Applied Research RCE test system is shown in Fig. 1. The brass cylindrical test specimens (1/2 inch dia. and 1/2 inch long) were machined from bar-stock. A freshly prepared specimen was used for each experiment and only its peripheral surface was exposed to the scale-forming solution. Additional details can be found elsewhere [21].

Analytical grade reagents $CaCl_2$ and Na_2SO_4 were dissolved in deionized water to produce $CaSO_4$ scale by co-precipitation. Concentration of each salt was kept at 0.03 mol/l. Equal volumes of the two solutions were mixed in a reservoir that was connected to glass test cell, to supply solution at rate of 1–1.5 l/h, so that the composition of scaling solution remains constant. Experiments were conducted on 120 and 600 grit polished cylindrical brass specimens at 60 and 70°C and atmospheric pressure for 6 h duration at various rotational speeds ranging from 100 to 2,000 revolutions per minute (RPM).

The surface texture of the 120 and 600 grit polished brass samples was determined by Bendix Linear Profile System (Model 5054). The measurements were performed at 20 ± 0.5°C and relative humidity of 40 ± 5%. The average roughness (R_a) of the test samples was measured both in forward and reverse direction.

An analytical balance with an accuracy of ±0.1 mg was used for weight measurements. The scaled sample was oven dried after each experiment. A minimum of triplicate experiments were performed at each temperature, surface roughness and rotational speed. The scale deposition rate was obtained by dividing the weight of scale obtained per unit area by the duration of the experiment. If deemed necessary, any abnormal point was repeated and the best of three were taken for the average deposition rate. The repeatability and uncertainty in the data generated was ±13%. The induction time was experimentally determined as a function of weight gain vs. time for each surface roughness and temperature used in the study.

Morphology of calcium sulfate crystals was studied on flat brass coupons (20 × 8 × 1.5 mm), polished to 120 and 600 grit with silicon carbide (SiC) emery paper. Duplicate specimens were assembled in a Teflon holder that was placed in the test cell and exposed to the calcium sulfate scale forming solution for 1–2 h under the same test conditions. After the tests, the coupons were retrieved, rinsed with distilled water, dried in an oven, and preserved for further examination. Scanning electron microscope (SEM) (JEOL JSM-5800-LV) was used for morphology study and the composition of scale was determined with energy dispersive X-ray spectrometer (EDS) coupled with the microscope.

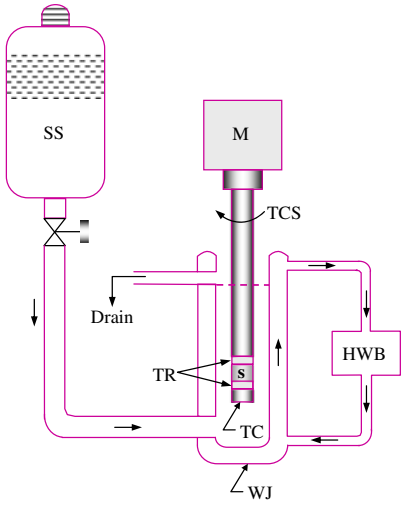

Fig. 1. Schematic of the experimental set-up of RCE equipment.
Notes: M=Motor to rotate specimen at fixed RPM, TCS =Teflon Coated Shaft, TR=Teflon Ring, S=Cylindrical Specimen, TC=Teflon Cap, HWB=Hot Water Circulation Bath, SS=Supersaturated Solution, WJ=Water Jacket.

3. Results and discussion

3.1. Surface roughness

The measured surface roughness (R_a value) of 120 and 600 grit polished brass samples by Linear Profile System, was 165 and 25 micro inch, respectively (Table 1). The lower value of R_a indicates a relatively smooth surface texture having less waviness compared to high value of R_a that refers to large peaks

Table 1
Average surface roughness (R_a) values of polished brass specimens

Surface polish (by SiC paper)	Measured average roughness R_a (μ inch)		Maximum average R_a (μ inch)
	Forward travel	Backward travel	
600 grit	22.5	25	25
120 grit	140	165	165

Note: Uncertainty: ± 4 μ inch, Conversion factor: 1 μ inch = 0.0254 μm.

and valleys of the rough surface profile. As can be seen from the table, the 120 grit polishing rendered more than five times the rough surface compared to 600 grit polishing. The brass is a soft material, hence, the big grits of 120 emery paper pierced more deeply into the specimens during polishing and produced a surface coarser than 600 emery paper.

3.2. Scale deposition

The induction period obtained experimentally (weight gain vs. time) for the 120 and 600 grit brass polished samples at 60°C was 40 ± 2 min and 35 ± 2 min, respectively, whilst at 70°C for 600 grit it was 30 ± 2 min.

Scaling/fouling is experienced in many industrial processes with normal or incompatible water or with dissolved inorganic salts in water, therefore, some of these salts and their compounds display inverse solubility characteristics [31] during operations because of creation of supersaturation. The calcium sulfate being an ionic compound has an inverse solubility behavior [31] which means that upon heating it becomes supersaturated, i.e. its concentration shoots up from the equilibrium (saturation) concentration and begins to precipitate immediately. Therefore, under favorable conditions such compounds can dissolve and form a significantly concentrated and highly ionized solution and start precipitating and depositing onto hot surfaces of equipment such as oil-producing wells, oil production facilities, and heat exchangers, consequently, forming a strongly adherent and mechanically resilient solid-phase deposits which are rock-like hard.

The major problem in scaling is the "choking or plugging" of oil production tubing (down hole and surface facilities) and loss of efficiency in heat exchangers. Hard scales may be physically removed by "scraping" or other mechanical means such as mechanized "pigging" or by chemical means such as acidization. The carbonate scales can be removed by acidizing treatment, whereas alkaline earth sulfate scales (such as calcium sulfate, magnesium sulfate, etc.) are impervious to standard acid treatment, therefore these strongly adhere to the metal surfaces and are rather difficult to remove.

The supersaturated solutions contain higher concentration of dissolved solutes than their equilibrium (saturated) concentration. Three possible states of supersaturation are represented schematically in Fig. 2. The solution is unstable in the labile zone, therefore, spontaneous precipitation can occur. In the stable regime, no precipitation can occur at all. In the metastable region (between the dotted and solid curves, Fig. 2), a solution may exist for long periods without precipitation occurring, but can become supersaturated upon heating or due to creation of favorable conditions. Thus, it is the boundary between the metastable and labile regimes (Fig. 2) that determines the occurrence of scaling in practical sense. Therefore, we selected solutes concentrations for our study such that the scaling solution remained in the metastable region below the supersolubility limit, and hence the scaling resulted only in the glass cell upon heating.

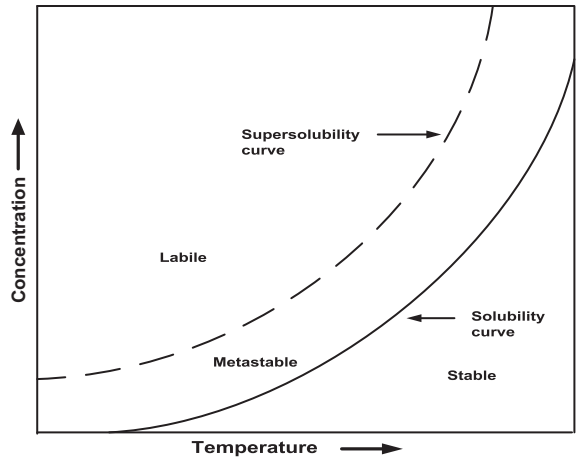

Fig. 2. A schematic representation of solution solubility and supersolubility (supersaturation) [3].

The agitation of supersaturated scaling solution due to the rotation of the specimen at various speeds had a strong impact on precipitation and the rate of mass transport of $CaSO_4$ scale to the electrode surface where it adsorbed and eventually deposited on the surface of the specimens and yielded measurable weight gain of scale on the brass substrate. The analysis of the data was carried out to demonstrate the impact of solution hydrodynamics on the deposition rate of scale. For this purpose, corresponding to each selected rotational speed in the study, the equivalent Reynolds number was calculated as suggested by Gabe [17].

The average scale deposition rates obtained at various Reynolds numbers are plotted in Fig. 3 to show the effect of Reynolds numbers on the deposition of calcium sulfate scale on 120 and 600 grit polished brass samples at 60 and 70°C, respectively. The results indicate an increase in the rate of deposition vs. Reynolds numbers, as shown by the best fit in the data generated in the study and are in agreement with the earlier studies [11,12,20–24].

Fig. 3 further shows the effect of surface finish of brass samples produced with 120 and 600 grit SiC emery papers. The 600 grit polished samples showed comparatively more scale than 120 grit polished samples at 60°C. The serrations or scratches on the 120 grit

polished surface were big enough (more rough) that they could not lock-in or incubate essentially the submicron incipient precipitating scale particles/crystals. Whereas on the contrary, the 600 grit polished surface texture was comparatively more appropriate for the incubation of embryonic scale crystallites which resulted in enhanced deposition on theses samples.

An increasing trend in the scaling rate for higher temperature of 70˚C is obvious from Fig. 3, as well. In addition, the deposition rate for 600 grit polished samples at the two selected temperatures of 60 and 70˚C can also be seen from the figure. At 70˚C, the rate of scale deposition marginally increased at the beginning but afterwards at higher Reynolds numbers ($\geq$ 500 RPM) it gradually decreased as compared to 60˚C for 600 grit polished brass samples (Fig. 3). A high rate of precipitation is always expected at increased temperature because of inverse solubility characteristics of the supersaturated solution [31]. But because the deposition of scale on specimen and the precipitation in bulk solution are two different processes [29], therefore, some variations are likely to occur in the deposition behavior due to high velocity (Reynolds numbers). The disparity seems to be the reason for the falling deposition rate of scale [31–33] on brass samples for higher Reynolds numbers at higher temperature of 70˚C, as portrayed in Fig. 3.

We kept the solution's ionic strength (chemistry) constant by replenishing fresh solution to the test cell and varied other parameters of interest, viz., temperature, surface roughness, and rotational speed. Although, scaling is a complex process, the following explanation, however, provides an overall process of scale deposition in a rather simple way.

The chemical equation governing the precipitation of scale from the supersaturated solution upon heating in the test cell can be presented as follows:

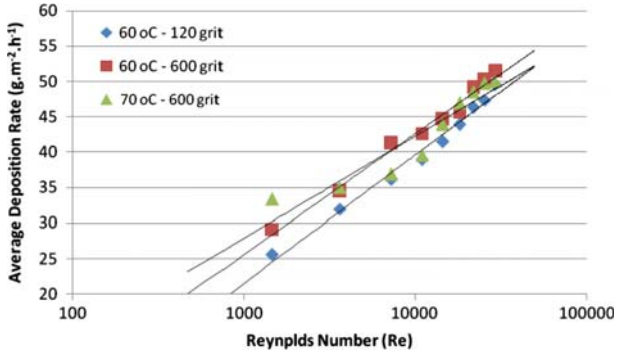

Fig. 3. Average deposition rate of calcium sulfate scale on 120 and 600 grit polished brass as a function of Reynolds Number at 60 and 70˚C.

$$Na_2SO_4\ (aq) + CaCl_2\ (aq) \rightarrow CaSO_4\ (s) + 2NaCl\ (aq) \quad (1a)$$

The reactants are ionic salts dissolved in water, so the above reaction in ionic form is:

$$Ca^{2+} + SO_4^{2-} + 2H^+ + 2OH^- \rightarrow CaSO_4{\cdot}2H_2O \quad (1b)$$

The resultant product $CaSO_4{\cdot}2H_2O$ (calcium sulfate dihydrate), the mineral called "gypsum," is the most commonly found sulfate scale in the oil production environment. The other forms of gypsum are: hemihydrate ($CaSO_4{\cdot}1/2H_2O$) and anhydrite ($CaSO_4$). All these forms of gypsum potentially cause scaling of oilfield equipment and fouling of heat exchanges. The $CaSO_4{\cdot}2H_2O$ is the most stable form of gypsum that occurs as sedimentary rock on the earth's crust. However the other forms, the hemihydrates ($CaSO_4{\cdot}1/2H_2O$) and anhydrite ($CaSO_4$) gypsum are also naturally found as rock, marble, plaster of Paris, alabaster, etc. in the earth's crust formations [3]. The combined water molecule (called water of crystallization) present in the hydrated gypsum can be evaporated upon heating at high temperature leaving behind anhydrous or dehydrated ($CaSO_4$) gypsum [3]. It is noteworthy that the $CaSO_4$ scale obtained in our study was identified earlier by XRD technique as hemihydrate gypsum [23].

The calcium cations (Ca^{2+}) and sulfate anions (SO_4^{2-}) join together to produce $CaSO_4$ as a precipitated solid-phase gypsum (Eq. (1)). Hundreds of thousands of submicroscopic crystals called nuclei of $CaSO_4$ precipitate which further coagulate (due to surface reaction) in the bulk of scaling solution and after gaining mass deposit on the active nucleation sites present on the surface of the specimen. The nucleation phenomena can be conceived as twofold during scale formation. The first nucleation is occurring in the bulk of the scaling solution due to onset of supersaturation and chemical reaction (Eq. (1)) while, the second nucleation is taking place on the surface of the specimen at active nucleation sites present because of surface heterogeneities (kinks, screw-dislocations, scratches, polishing marks, etc.). These surface irregularities are low energy sites, which attract the precipitating species (diffusion and adsorption) which finally adhere at these active sites on the surface of metal due to mechanical bonding as scale (Physics). In addition, the suspended solids, corrosion products, bio-mass, sludge and slime in the flow system can also play an important role in promoting the scale deposition process.

A simplified schematic representation of the scale deposition mechanism resulting from cooling water

system or process fluid stream is shown in Fig. 4. The figure shows that the scale deposition is characterized by the dissolution of minerals salts in water, supersaturation of dissolved salts, nucleation, precipitation, adherence and growth, surface characteristics and contact time. The heterogeneous (spontaneous) precipitation or crystallization is occurring because of high concentration, high temperature, external seeding, contamination, and particulate matters. The homogeneous precipitation is happening in case of pure salt (s) in low or moderate concentrations without any seeding or pollution. We used pure solutes in low concentration at moderate temperature to deposit single salt $CaSO_4$ which followed the homogeneous crystallization path (Fig. 4) in the reported study.

The replenishment of the fresh solution to the test cell provided constant ionic potential so that the chemical reaction never ceased and continuously produced precipitation in the bulk solution in our study. However, at high rotational speeds, shear forces increase at the solid–liquid interface, so the scale erosion (removal) process may become significant along with the scale deposition process. Therefore, there is always a competing effect between these two contending (deposition and removal) phenomena occurring simultaneously and ultimately the precedence shifts towards the dominant part during the fluid flow system. Secondly, at high rotation (high velocity), the contact time of scale to the surface of specimens becomes less. This may be the reason that the rate of scale deposition comparatively rips off at higher rotational speeds, as already illustrated in Fig. 3.

In certain cases, the turbulence at high rotations (flow velocity) may act as a means of scale removal due to high shear forces, that may wash away the freshly depositing layers of scale on the previously deposited scale (i.e. reverse of deposition process under favorable conditions due to high velocity). We observed breaking away of some tiny pieces of scale in the glass cell at high rotational speeds ($\geq$1,500 RPM), which may be due to scale removal process. Another reason could be that since the $CaSO_4$ crystals growth is of acicular form (see morphology section), therefore, the crystals are prone to break away, wash away or even dislodge at high velocity. This pertinent mechanistic behavior (growth and dissolution) from incompatible waters or supersaturated solutions can briefly be summarized as follows:

- creation of supersaturation and precipitation,
- diffusion and transport of scaling species to the substrate surface,
- adsorption of scalant on the substrate surface to form "adions,"
- incorporation of adions into the surface lattice of metal/previous scale layer, and
- dissolution or removal process if favorable conditions exist (e.g. high velocity).

Fig. 5 presents a comparison, under identical experimental conditions, between the deposition rate of $CaSO_4$ scale on brass and stainless steel-316 [21]. The brass substrate shows comparatively more scale deposition than stainless steel-316 at lower Reynolds num-

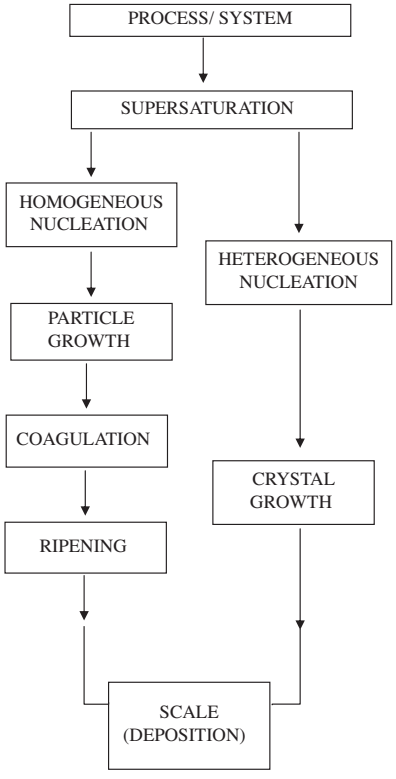

Fig. 4. Schematic representation of the scale deposition mechanism from process water/fluid system.

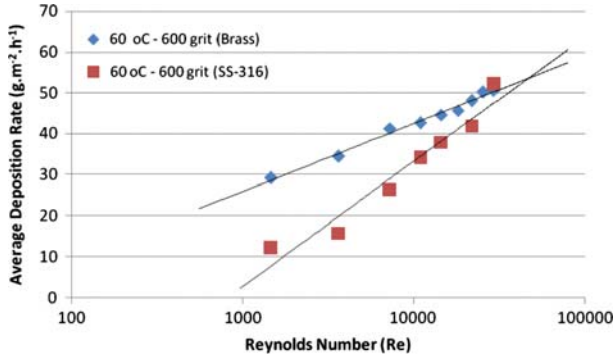

Fig. 5. Comparison of average deposition rate of calcium sulfate scale on brass and SS-316 [21].

bers but at higher Reynolds numbers the deposition on brass drops off and becomes less than SS-316. This anomaly can be attributed partly to the scale removal process which attains dominance at higher Reynolds numbers and partly to material characteristics such as surface activation energy and/or surface wetness. Therefore, the trend for the deposition of scale on brass was not favorable compared to stainless steel so brass in general showed an overall falling scale deposition rate [31–33] compared to SS-316 (Fig. 5).

We used pure salts without any external seeding or contamination in the present study. The seeding enhances the crystallization process [5–7]. The external impurities such as particulates, suspended solids, mixed salts, corrosion products, biological matters, surface geometry and flow velocity, etc. play a significant role on the deposition behavior of scale on the substrate and affects the overall growth rate of scale. If these conditions exist, the scaling/fouling rate may result in increasing, falling or asymptotic relationships [31–33]. In heat exchange equipment the asymptotic behavior of scaling/fouling is observed when the rate of deposition of scale is equal to the rate of removal of scale under appropriate fluid flow conditions.

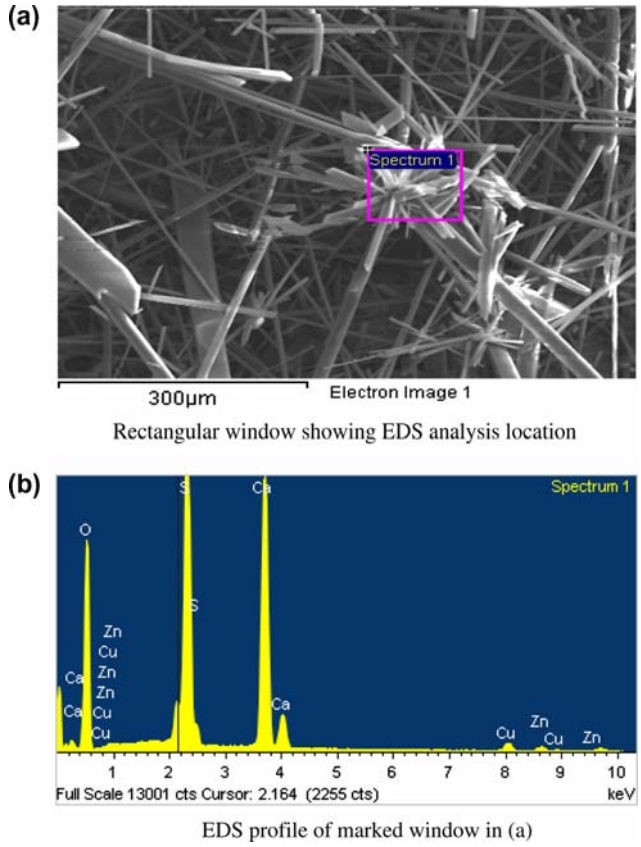

Fig. 6. EDS spectra of calcium sulfate scale crystals deposited on brass (copper and zinc alloy elements).

3.3. Morphology

The SEM examination of the gypsum scale exhibited acicular (needle-, rods-like) crystals growth. However, at certain locations some flat crystals were also seen which had been formed due to the coagulation of prismatic rods. The SEM examination in general showed that the $CaSO_4$ crystals initially emerged at the nucleation sites on the substrate surface or on the existing crystals and then branched out randomly in all directions. The EDS profile obtained at a particular location on scaled brass specimen is shown in Fig. 6. The scale forming solution was prepared from pure chemicals, therefore, the large peaks for calcium (Ca), sulfur (S), and oxygen (O) in the EDS spectra confirmed the nature of crystals as calcium sulfate ($CaSO_4$). The small peaks for Cu and Zn are the constituents of brass (alloy of copper and zinc).

Fig. 7 presents some typical SEM morphological results of calcium sulfate crystals deposited on brass substrate from the scale-forming solution. The results show that the scale crystals initially grow at the nucleation sites in the shape of tiny prisms which further develop into needles or prismatic rods and then coalesce together to form flat crystals The photomicrographs in Fig. 7(a) and (c) show a dense population of uniformly distributed CaSO4 crystals on the entire surface of the brass substrate. Similar results were obtained in earlier studies for the $SrSO_4$ [8], $BaSO_4$ [20] and $CaSO_4$ [21–24] scale deposition on stainless steel-316, copper, and aluminum. The micrographs, however, further indicate the random growth of subsequent crystals emanating from either the nucleation sites or the already deposited primary crystals. In addition, the secondary as well as perpendicular growth of $CaSO_4$ crystals is also evident in these micrographs (Fig. 7(a)–(d)). Fig. 7(b) presents an enlarged view of the central portion of Fig. 7(a) and (c) shows the flower type random nucleation growth, as well. The crystals thus seem to have been growing at preferential nucleation sites available on the substrate and/or previously deposited scale layer.

It is speculated that once an initial layer of scale is formed the subsequent scale growth on it is much faster because of the readily available abundant nucleation sites as compared to a polished surface during scale deposition process on metal surface. The scaled surface becomes sufficiently rough with large surface area, which subsequently promotes deposition as compared to a bare or polished surface. The existing layers of scale provide more nucleation sites for further

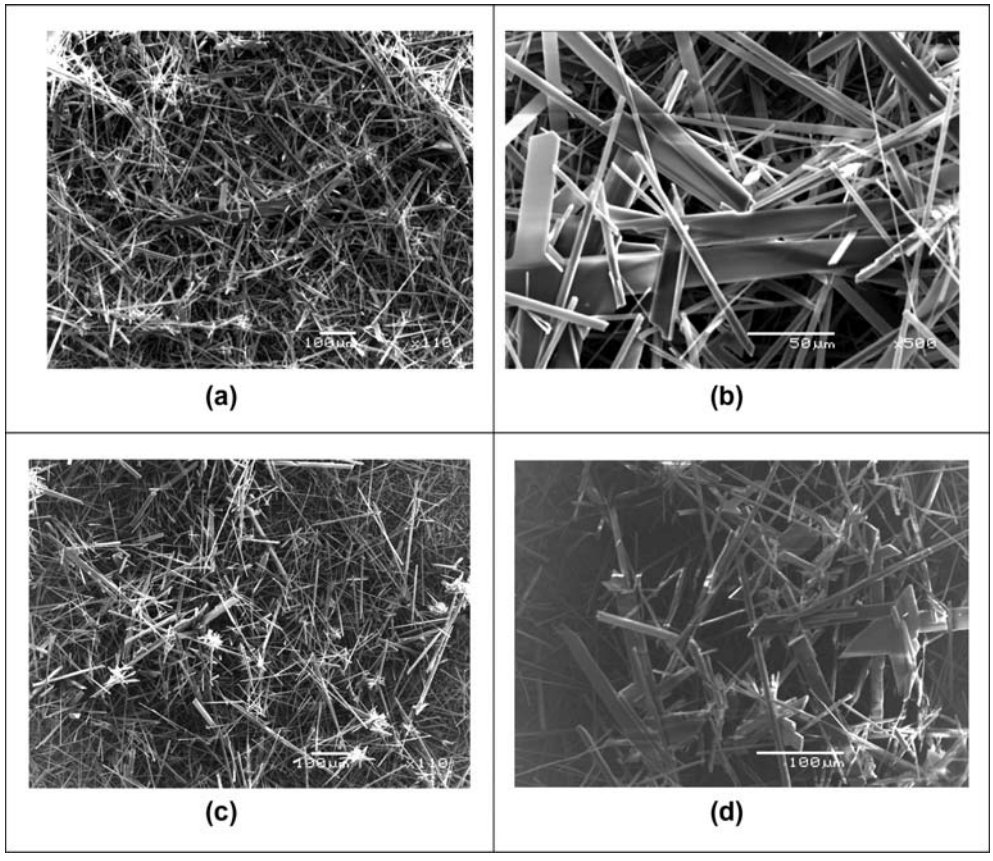

Fig. 7. SEM micrographs showing the morphology and distribution of $CaSO_4$ crystals on brass substrate. General morphology (a–d): prismatic needles, rods, flat plates, random, perpendicular and secondary growth at nucleating sites. (b) Shows enlarged view of middle portion of micrograph-(a) at 500×.

scale growth and adhesion on the substrate surface. These morphological results agree with the earlier studies [8,20–24]. The reason seems to be a random growth of the subsequent crystallites on the previously deposited scale crystals, i.e. a sort of epitaxial growth, as revealed from the SEM micrographs (Fig. 7), which promotes scale deposition process.

4. Conclusions

The replenishment of scaling solution to the test cell provided constant ionic chemistry for the scale precipitation and deposition throughout the experiments.

The turbulence generated due to the agitation of the solution promoted scale formation by allowing more active scaling species to adsorb on the metal surface that eventually deposited and adhered on brass substrate. The hydrodynamics of solution plays a vital role in scale deposition process, therefore, it must be an integral part of any water treatment, scale squeeze or prognostic model.

The effect of surface roughness on the deposition of calcium sulfate scale on brass was conspicuous. The 120 grit polished samples showed comparatively less scale than 600 grit polished brass specimens.

The deposition of calcium sulfate scale rate on brass was higher than SS-316 but it showed an overall falling rate as compared to stainless steel-316 under identical test conditions.

The effect of temperature increase was significant on scale deposition because of the inverse solubility effect of supersaturated scaling solution. At 70˚C more deposition of calcium sulfate scale on brass was observed at the beginning, but due to the competing effect between scale deposition and removal, the removal process became dominant and the rate comparatively dropped off at higher Reynolds numbers than at 60˚C under the same test conditions.

The scale deposition rate vs. Reynolds number showed increasing trend for the data developed in the present work; however, in practical industrial situations, the deposition may likely show a different behavior, e.g. falling or asymptotic rate.

The SEM examination revealed prismatic needles, rods, and flat crystal structures. The growth of $CaSO_4$ crystals initially started at the nucleation sites present on the specimen surface and then branched out randomly in all directions. Perpendicular growth and flower-shaped crystals emanating from nucleating sites were evident at certain locations. In addition, growth of secondary crystals of scale on the primary crystals was also observed from SEM micrographs.

Acknowledgement

The support of the Ministry of Higher Education and the Research Institute of King Fahd University of Petroleum and Minerals for this work is highly acknowledged.

Symbols

R_a	—	average surface roughness (μ inch)
Re	—	Reynolds number (dimensionless)
aq	—	aqueous
s	—	solid

References

[1] R. Steinhagen, H. Muller-Steinhagen, K. Maani, Problems and costs due to heat exchanger fouling in New Zealand industries, Heat Transfer Eng. 14(1) (1992) 19–30.
[2] D.E. Potts, R.C. Ahlert, S.S. Wang, A critical review of fouling of reverse osmosis membranes, Desalination 36 (1981) 235–264.
[3] J.C. Cowan, D.J. Weintritt (Eds.), Water Formed Scale Deposits, Gulf, Houston, TX, 1976.
[4] M. Al-Ahmed, F.A. Aleem, Scale formation and fouling problems effect on the performance of MSF and RO desalination plants in Saudi Arabia, Desalination 93 (1993) 287–310.
[5] P.A. Read, J.K. Ringen, The use of laboratory tests to evaluate scaling problems during water injection, SPE 10593, presented at 6th International Symposium on Oilfield and Geothermal Chemistry, Dallas-Taxes, January 25–27, 1982, pp. 7–17.
[6] G.H. Nancollas, The growth of crystals in solution, Adv. Colloid Interface Sci. 10 (1979) 215–252.
[7] Sung-Tsuen Liu, G.H. Nancollas, The kinetics of crystal growth of calcium sulfate dihydrate, Cryst. Growth 6 (1970) 281–289.
[8] M.I. Khokhar, S.K. Somuah, M.O. Amabeoku, I.M. Allam, A. Quddus, Oilfield scaling—mechanism of formation, Proc. 4th Middle East Corrosion Conference, Bahrain, January 11–13, 1988, Part 1, pp. 244–258.
[9] S.M. Zubair, A.K. Sheikh, M.O. Budair, M.U. Haq, A. Quddus, O.A. Ashiru, Statistical aspects of $CaCO_3$ fouling in AISI 316 stainless steel tubes, Heat Tran. (Trans. ASME) 119 (1997) 581–588.
[10] M.O. Budair, M.S. Sultan, S.M. Zubair, A.K. Skiekh, A. Quddus, $CaCO_3$ Scaling in AISI 316 tubes—effect of thermal and hydraulic parameters on the induction time and growth rate, Heat Mass Transf. 34 (1998) 163–170.
[11] D. Hasson, M. Avriel, W. Resnick, T. Rosenman, S. Windreich, Mechanism of calcium carbonate scale deposition on heat-transfer surfaces, I EC Fundam. 7(1) (1968) 59–65.
[12] D. Hasson, J. Zahavi, Mechanism of $CaSO_4$ scale deposition on heat transfer surfaces, I EC Fundam. 9(1) (1970) 1–10.
[13] G. Liu, D.A. Tree, M.S. High, Relationship between rotating disk corrosion measurements and corrosion in pipe flow, Corrosion 50 (1994) 584–593.
[14] K.D. Efrid, E.J. Wrright, J.A. Boros, T.G. Hailey, Correlation of steel corrosion in pipe flow with jet impingement and rotating cylinder tests, Corrosion 49 (1993) 992–1003.
[15] D.C. Silverman, Rotating cylinder electrode for velocity sensitive testing, Corrosion 40 (1984) 220–226.
[16] D.C. Silverman, Rotating cylinder electrode—geometry relationships for prediction of velocity—sensitive corrosion, Corrosion 44 (1988) 42–49.
[17] D.R. Gabe, The rotating cylinder electrode, Appl. Electrochem. 4 (1974) 91–108.
[18] O.A. Ashiru, J.P.G. Farr, Kinetics of reduction of silver complexes at the rotating disk electrode, Electrochem. Soc. 139 (10) (1992) 2806–2810.
[19] C.T.J. Low, C.P. de Leon, F.C. Walsh, The rotating cylinder electrode (RCE) and its application to the electrodeposition of metals, Aust. Chem. 58 (2005) 246–262.
[20] A. Quddus, I.M. Allam, $BaSO_4$ scale deposition on stainless steel, Desalination 127 (2000) 219–224.
[21] A. Quddus, Effect of hydrodynamics on the deposition of $CaSO_4$ scale on stainless steel, Desalination 142 (2002) 57–63.
[22] A. Quddus, L.M. Al-Hadhrami, Hydrodynamically deposited $CaCO_3$ and $CaSO_4$ scales, Desalination 246 (2009) 526–533.
[23] L.M. Al-Hadhrami, A. Quddus, Role of solution hydrodynamics on the deposition of $CaSO_4$ scale on copper substrate, Desalin. Water Treat. 21 (2010) 238–246.
[24] A. Quddus, L.M. Al-Hadhrami, Influence of solution hydrodynamics on the deposition of $CaSO_4$ scale on aluminum, Thermophys. Heat Tran. 25(1) (2011) 112–118.
[25] A. Neville, A.P. Morizot, T. Hodgkiess, Electrochemical aspects of surface/solution interactions on scale initiation and growth, Mater. Performance 37(5) (1998) 50–57.
[26] A. Neville, A.P. Morizot, T. Hodgkiess, Electrochemical assessment of $CaCO_3$ deposition using a rotating disc electrode, Appl. Electrochem. 37(4) (1999) 455–462.
[27] A. Neville, A.P. Morizot, Calcareous scale formed by cathodic protection—an assessment of characteristics and kinetics, Cryst. Growth 345 (2002) 490–502.
[28] A. Morizot, A. Neville, T. Hodgkiess, Studies of deposition of $CaCO_3$ on a stainless steel surface by a novel electrochemical technique, Cryst. Growth 198(199) (1999) 738–743.
[29] T. Chen, A. Neville, M. Yuan, Calcium carbonate sclae formation—assessing the initial stages of precipitation and deposition, Petrol. Sci. Eng. 46 (2005) 185–194.
[30] R.P. Singh, N.M. Abbas, Characterization of oilfield scales, Proc. 5th Middle East Corrosion Conference, Bahrain, October 28–30, 1991, Vol. 4, pp. 561–569.
[31] T.R. Bott, Fouling of Heat Exchangers, Elsevier, Netherlands, 1995.
[32] G.F. Hewitt (Ed.), Hemisphere Handbook of Heat Exchanger Design, Section 3.17, Hemisphere, New York, NY, 1990.
[33] J.G. Knudsen, Cooling water fouling—a brief review, Proc. The 20th ASME/AIChE Heat Transfer Conference, Milwaukee-Wisconsin, August 2–5, 1981, HTD-Vol. 17, pp. 29–38.